

# A theoretical study of the optical properties of nanostructured TiO<sub>2</sub>

Q.1 Valeria C Fuertes<sup>1,2</sup>, Christian F A Negre<sup>1,3</sup>, M Belén Oviedo<sup>1</sup>, Franco P Bonafé<sup>2</sup>, Fabiana Y Oliva<sup>2</sup> and Cristián G Sánchez<sup>1</sup>

(Ed: Emily)

<sup>1</sup> Departamento de Matemática y Física, Facultad de Ciencias Químicas, INFIQC, Universidad Nacional de Córdoba, Ciudad Universitaria, X5000HUA, Córdoba, Argentina

<sup>2</sup> Departamento de Físicoquímica, Facultad de Ciencias Químicas, INFIQC, Universidad Nacional de Córdoba, Ciudad Universitaria, X5000HUA, Córdoba, Argentina

<sup>3</sup> Department of Chemistry, Yale University, New Haven, CT 06520-8107, USA

Q.2 E-mail: [cgsanchez@fcq.unc.edu.ar](mailto:cgsanchez@fcq.unc.edu.ar)

Received 29 October 2012, in final form 29 December 2012

Published

Online at [stacks.iop.org/JPhysCM/25/000000](http://stacks.iop.org/JPhysCM/25/000000)

Ascii/Word/JPCM/  
cm451385/PAP

Printed 4/2/2013

Spelling US

Issue no

Total pages

First page

Last page

File name


Date req

Artnum

Cover date

## Abstract

Optical properties of TiO<sub>2</sub> nanoclusters (with more than 30 TiO<sub>2</sub> units) were calculated within a fully atomistic quantum dynamic framework. We use a time dependent tight-binding model to describe the electronic structure of TiO<sub>2</sub> nanoclusters in order to compute their optical properties. We present calculated absorption spectra for a series of nanospheres of different radii and crystal structures. Our results show that bare TiO<sub>2</sub> nanoclusters have the same adsorption edge for direct electronic transition independently of the crystal structure and the nanocluster size. We report values of the adsorption edge of around 3.0 eV for all structures analyzed. In the present work we demonstrate that, for small clusters, both the direct transition absorption edge and the blue shifting phenomena are masked by thermal disorder.

 Online supplementary data available from [stacks.iop.org/JPhysCM/25/000000/mmedia](http://stacks.iop.org/JPhysCM/25/000000/mmedia)

Q.3 (Some figures may appear in colour only in the online journal)

Q.4 TiO<sub>2</sub> composed nanomaterials are currently used in a wide range of applications. Paints, toothpaste, photocatalysts, photovoltaic sensors and UV protectors are among the materials that employ TiO<sub>2</sub> as the active component [1–6]. The singular properties of these materials are mainly based on the optical features of TiO<sub>2</sub> arising from its band gap (BG) structure [7]. When coated with organic dyes or inorganic narrow band gap semiconductors, TiO<sub>2</sub> nanoparticles can absorb light into the visible region, which makes them suitable for use in dye sensitized solar cells (DSSC) [8–11].

Q.5 TiO<sub>2</sub> is present in nature in three main phases: rutile, anatase and brookite. Unit cells for these three TiO<sub>2</sub> polymorphs are shown in figure 1. These structures can be described in terms of chains of TiO<sub>6</sub> octahedra, where each Ti<sup>4+</sup> ion is surrounded by six O<sup>2-</sup> ions in the positions of octahedral vertices. The three crystal structures differ in the distortion of each octahedron and the assembly pattern of the chains. Differences in lattice structures are responsible for different mass densities and electronic band structures

among the three forms of TiO<sub>2</sub>. The rutile phase is the most stable as a bulk material. At very small particle dimensions, when surface energy becomes the most important component of the total energy, anatase (which produces fewer spherical particles) becomes the most stable structure [12]. However, relative stabilities of different nanostructured phases may depend on several factors such as pressure and chemical environment [13, 14].

Optical properties of TiO<sub>2</sub> nanoparticles have been the subject of intensive studies involving a variety of spectroscopic techniques [7]. Important absorption features, such as the adsorption edge determined with UV–visible spectroscopy, are directly related to the structure of the BG. The valence band for both bulk and nanostructured TiO<sub>2</sub> is composed of 3d Ti and 2p O states with the conduction band edge composed mainly of 3d Ti states [7]. TiO<sub>2</sub> nanomaterials usually have electronic BGs larger than 3.0 eV with high absorption intensity in the UV region. The main mechanism of light absorption in pure semiconductors is by

Q.6

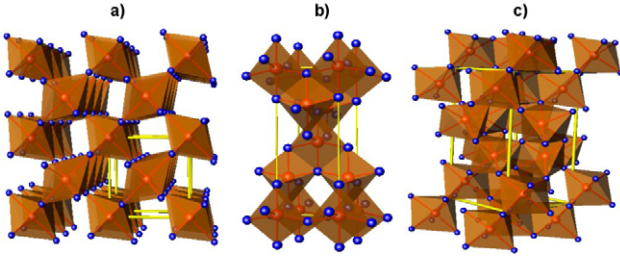


**Figure 1.** Crystal structures of TiO<sub>2</sub> polymorphs. Red spheres are Ti<sup>4+</sup>, blue spheres are O<sup>2-</sup> and yellow lines represent the unit cell. (a) Rutile. (b) Anatase. (c) Brookite.

direct inter-band electron transitions; therefore, a detailed knowledge of the BG energy of TiO<sub>2</sub> nanostructures is of fundamental importance. DSSC applications, for example, require understanding the structure of the bands related to the size and shape of the nanostructure [8]. Among the unique properties of semiconductors, the movement of electrons and holes is primarily influenced by the well-known quantum confinement effect, which, in turn, is greatly affected by the size and geometry of the materials [15–18].

Some experimental and theoretical evidence suggests a slight blue shift of the absorption edge of nanostructured TiO<sub>2</sub> as compared to the bulk material [19–24]. This is mainly due to an increase in the BG, which is a consequence of the reduction in size [25]. Whether there is or is not an optical shift in the TiO<sub>2</sub> nanoparticle absorption edge has been the subject of intensive discussions from the first work introducing this phenomenon [19, 26] to analytical calculations involving surface properties [27]. The question of the threshold in cluster size that separates the optical properties of nanoparticles from those of the bulk material is one that remains unanswered. It is very difficult to predict the optical shifts of small TiO<sub>2</sub> nanoparticles (<190 TiO<sub>2</sub> units). This is probably because surface reconstructions perturb the electronic structure, complicating the interpretation of the usual trends [27]. As part of the conclusion of this work we may say that the Brus formula [25] commonly used to estimate particle size from absorption edge shift is no longer applicable when particles are small and the rearrangement of the surface is significant.

From the point of view of theoretical calculations, the use of purely *ab initio* methods such as Hartree–Fock or density functional theory (DFT) ones for molecular or periodic systems shows different results depending on the method. Despite the fact that DFT provides excellent results for ground state (GS) properties, calculations involving excited states may sometimes suffer from an incomplete treatment of electron correlation, leading to the underestimation of BGs in TiO<sub>2</sub> polymorphs [28–31]. On the other hand, explicitly correlated methods, such as the *GW* one, overestimate the BG energy [32, 33]. As an alternative to these methods, a time dependent self-consistent density functional tight-binding (TD-DFTB) method can yield results that take into account the renormalization of the BG (with respect to the HOMO–LUMO energy difference) but with less computational cost, allowing the study of larger systems

(with more than 30 TiO<sub>2</sub> units) [34]. The aim of the current work is to calculate the absorption spectra of relatively large TiO<sub>2</sub> (190 > TiO<sub>2</sub> units > 30) nanoparticles by using a fully quantum dynamical method based on TD-DFTB. By using this method, trends of the absorption features upon varying the size and crystal structure of the aforementioned TiO<sub>2</sub> nanoclusters were determined. However, the nanoparticles studied here have a sizes in between those of small TiO<sub>2</sub> clusters for which the structure has been crystallized [35], and large particles which show well defined crystal faces (lower energy crystalline habits) [36].

## 1. The computational method

A self-consistent density functional tight-binding method (SCC-DFTB) was used to describe the electronic structure of the clusters [37]. This method is based on a second-order expansion of the Kohn–Sham energy functional around a reference density of neutral atomic species [37]. The DFTB+ computational code [38] which implements SCC-DFTB has been used to compute the Hamiltonian and overlap matrix elements and the initial single-electron density matrix. For the calculations performed here, we have used the tiorg-0-1 Slater–Koster parameter set for the description of TiO<sub>2</sub> which has been validated in [34].

The methodology applied for calculating optical properties based on TD-DFTB has been recently published in [39, 40] and is based on the propagation of the one-electron density matrix for further computing the frequency dependent polarizability.

Briefly described, this technique introduces an initial perturbation in the shape of a Dirac delta pulse ( $\hat{H} = \hat{H}^0 + E_0\delta(t - t_0)\hat{\mu}$ ) to the initial GS density matrix previously obtained [41]. After the pulse application, the density matrix evolves in time and its evolution can be calculated by time integration of the Liouville–Von Neumann equation of motion in the non-orthogonal basis.

$$\frac{\partial \hat{\rho}}{\partial t} = \frac{1}{i\hbar} (S^{-1} \hat{H}[\hat{\rho}] \hat{\rho} - \hat{\rho} \hat{H}[\hat{\rho}] S^{-1}) \quad (1)$$

where  $\hat{H}$  is the Hamiltonian matrix,  $S$  is the overlap matrix and  $\hat{\rho}$  is the density matrix. For all the calculations below, time step integration was set to  $9.675 \times 10^{-4}$  fs and  $E_0 = 0.01$  V Å<sup>-1</sup>. In the linear response regime, when the applied electric field pulse is small, the response is linear and the dipole moment is

$$\mu(t) = \int_{-\infty}^{\infty} \alpha(t - \tau) E(\tau) d\tau \quad (2)$$

where  $E(\tau) = E_0\delta(\tau - \tau_0)$  is the initial perturbation mentioned before, and  $\alpha(t - \tau)$  is the polarizability along the axis over which the external field  $E(t)$  is applied. The absorption spectrum is proportional to the imaginary part of the frequency dependent polarizability, obtained from the Fourier transform of the time dependent dipole moment, after deconvolution of the applied electric field

$$\alpha(E) = \frac{\mu(E)}{E_0}. \quad (3)$$

The average of the polarizability along the three Cartesian axes is taken as the absorption spectrum of the system.

In previous publications [39] we have studied the absorption spectra of chlorophylls with TD-DFTB. In these previous manuscripts we showed that TD-DFTB based spectra showed a remarkable agreement with the experiment, even better than the ones obtained by TD-DFT, probably due to a compensation of errors.

## 2. Results and discussion

### 2.1. $\text{TiO}_2$ cluster generation

In this section we will briefly describe the method used to generate input structures for the optical calculations.  $\text{TiO}_2$  nanoclusters are generated by performing molecular dynamic simulations. We first construct a bulk piece from lattice points following the arrangements of the conventional unit cell for anatase, rutile and brookite. After that, we cut spherical nanostructures by taking the lattice points that are inside a desired radius. The procedure then follows by replacing the lattice points with the appropriate lattice base for each polymorph.

Once the base is replaced at every lattice point, we obtain a cluster with a highly anisotropic surface with an excess of O atoms in a particular orientation. An annealing Monte Carlo method was employed to reorder the atoms of the surface in order to produce a better input for the molecular dynamics; a description of this procedure is included in the supporting information (available at [stacks.iop.org/JPhysCM/25/000000/mmedia](http://stacks.iop.org/JPhysCM/25/000000/mmedia)).

The LAMMPS code has been used to perform MD simulations [42]. In the case of  $\text{TiO}_2$  modeling, we have used the Matsui–Akaogi potentials detailed in [43]. These potentials are highly reliable and have been utilized in several previous structural  $\text{TiO}_2$  analyses [12–14, 44–47].

MD simulations were carried out in the canonical ensemble ( $NVT$ ) at 300 K for 3.5 ns of production time using a time step of 3.5 fs after adequate equilibration. From a thermodynamic point of view, small rutile and brookite clusters should transform into anatase, but no phase transition can occur in the simulation time scale [12]. This was verified by checking radial distribution functions during the MD runs (see figure 2). To perform all optical calculations, we have taken eleven frames of the last 500 000 steps of production run separated by 50 000 MD steps. Particle coordinates produced by this method are between 14 Å diameter for the smallest cluster (a rutile cluster of 30  $\text{TiO}_2$  units) and 23.5 Å diameter for the largest (190  $\text{TiO}_2$  units of anatase). This radius is estimated by taking the distance from the center of mass to the farthest atom. Figure 2(d) shows a picture of the coordinates of the last frame of the MD for the largest particle analyzed here. We have seen that smaller particles cannot host a conventional lattice cell within, and larger particles than those for which results are presented here are too computationally demanding for optical calculations. From looking at the conventional cell of each polymorph it is fair to say that for defining an anatase, rutile or brookite cluster

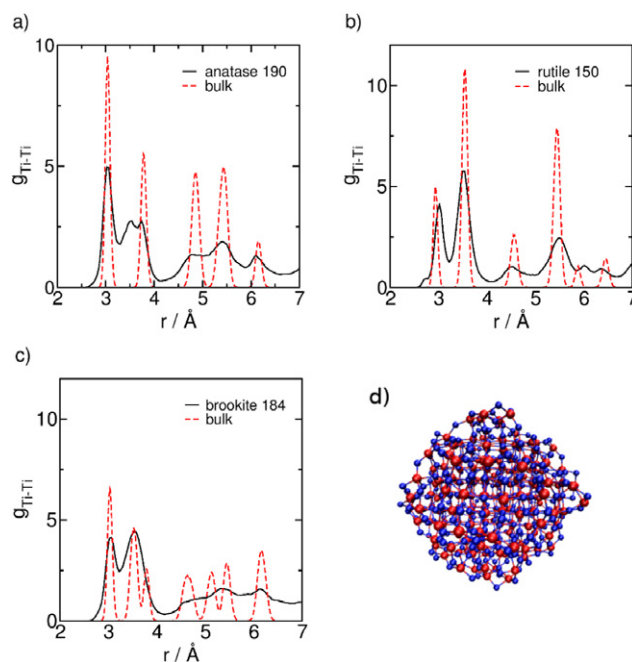


**Figure 2.** Ti–Ti radial distribution functions for the three  $\text{TiO}_2$  structures compared to the bulk: (a) 190  $\text{TiO}_2$  units of anatase; (b) 150  $\text{TiO}_2$  units of rutile; (c) 184  $\text{TiO}_2$  units of brookite; (d) structure representation of a cluster of 190  $\text{TiO}_2$  units of anatase. Red and blue spheres represent Ti and O atoms respectively.

we should have at least 13, 9 or 8  $\text{TiO}_2$  units respectively. This work is complementary to [32] in the sense that we start optical properties studies at sizes where clusters are large enough to possess a defined interior crystal structure.

From looking at the radial distribution functions shown in figure 2, we can be assured that, despite the clusters being maintained at 300 K, they show a characteristic structure which is similar to the corresponding bulk counterpart. We can see that the heights of the first two peaks have different behaviors for each cluster. In the case of brookite, the two peaks are of roughly the same height (black line of figure 2(c)). In the case of rutile, the second peak is higher than the first one, and the inverse holds for anatase. Radial distribution functions determined here are in fair agreement with those shown in [14].

### 2.2. Optical properties

We have computed the absorption spectra for the clusters obtained with the aforementioned procedure (figure 3). Each absorption spectrum is computed by averaging eleven spectra obtained from the frame selection mentioned before. The overall spectral shapes are in good agreement with those shown in [29, 48].

Studies of the surface/volume ratio and sphericity parameter ( $\zeta$ ) as shown in tables S3 and S4 in the supporting information (SI available at [stacks.iop.org/JPhysCM/25/000000/mmedia](http://stacks.iop.org/JPhysCM/25/000000/mmedia)) show that these particles are not perfectly spherical, brookite and anatase being the least and most spherical ones respectively. The range of sizes studied in this

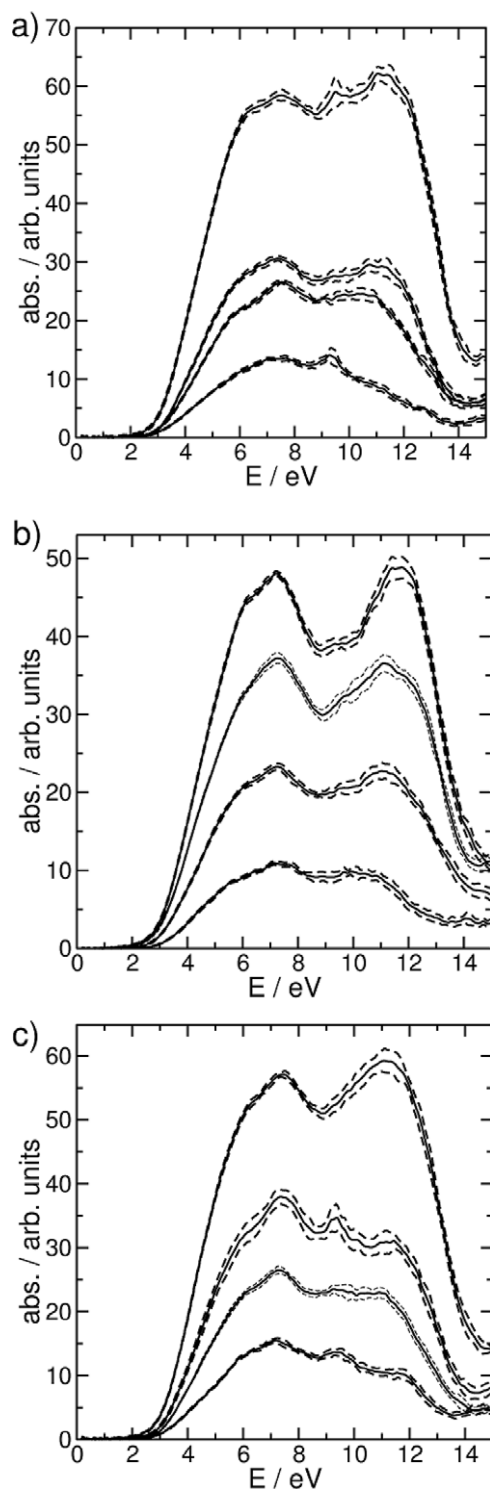


**Figure 3.** Calculated spectra. (a) Anatase: 34, 74, 90 and 190  $\text{TiO}_2$  units; (b) rutile: 30, 74, 118 and 150  $\text{TiO}_2$  units; (c) brookite: 40, 72, 104, and 184  $\text{TiO}_2$  units. Dashed lines show the  $\pm$  standard deviation boundaries.

paper lies in between small  $\text{TiO}_2$  nanoclusters, where the crystalline structure is perfectly known [35], and large NPs (larger than 50 nm), for which the shape is known to arise from minimizing the surface energy by exposing the most energetically favorable faces. In this sense, we are addressing optical properties for sizes that are currently unexplored.

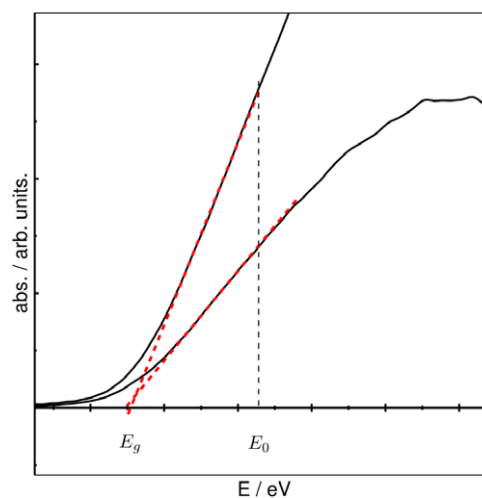


**Figure 4.** Fitting procedure for two different cluster sizes: the red dashed line indicates a linear fit approximating the graph at the inflexion point ( $E_0$ ). The absorption edge ( $E_g$ ) is determined as the intercept of the linear fit with the energy ( $E$ ) axis.

From figure 3, it can be seen that these clusters have a strong absorption band in the UV region which extends between 3 and 15 eV with, in most cases, a depletion at 8 eV. The strongest depletion is observed for the case of rutile. The same feature appears in the experimental measurements shown in [29]. Except for the largest cluster of the brookite set (figure 3(c)), the overall shape of this broad band is quite conserved for all polymorphs.

Anatase and brookite absorb 35% and 30% respectively per  $\text{TiO}_2$  unit more than rutile in the region under 15 eV, and this is consistent with the trends of the volume of the unit cell (the mass density) of each polymorph.

In order to properly determine the absorption edge we proceeded by fitting the region between 0 and 6.5 eV of each spectrum with a Chebyshev polynomial of degree 13. The use of orthogonal polynomials as a fitting basis ensures proper convergence of the fitting procedure and no over-fitting of noisy features [49]. After this, the absorption edge ( $E_g$ ) is found as the energy value of the intercept with the energy axis of the tangent line at the inflexion point  $E_0$  of the polynomial. This tangent line is determined analytically from the fit. A pictorial representation of this procedure is shown in figure 4. Average values for  $E_g$  together with their standard deviations over the eleven spectra samples are shown in table 1.

As shown in table 1, absorption edges found by using this procedure are almost the same for all the clusters analyzed here with an average value of around 3.0 eV. This value is close to the rutile bulk value which is 3.00 eV (for anatase and brookite the  $E_g$  bulk values are 3.21 and 3.13 eV respectively) [29]. Results for absorption edges calculated here are in fair agreement with those for the largest clusters analyzed in [50, 51]. In the present work, there is no evidence of any significant differences of the  $E_g$  compared between different polymorphs. Moreover, there is no blue shift as the NPs become smaller. This was also suggested by other experimental and computational results [50].



**Table 1.** Calculated average  $E_g$  values for all the clusters considered in this work together with standard deviations over the calculated spectra.

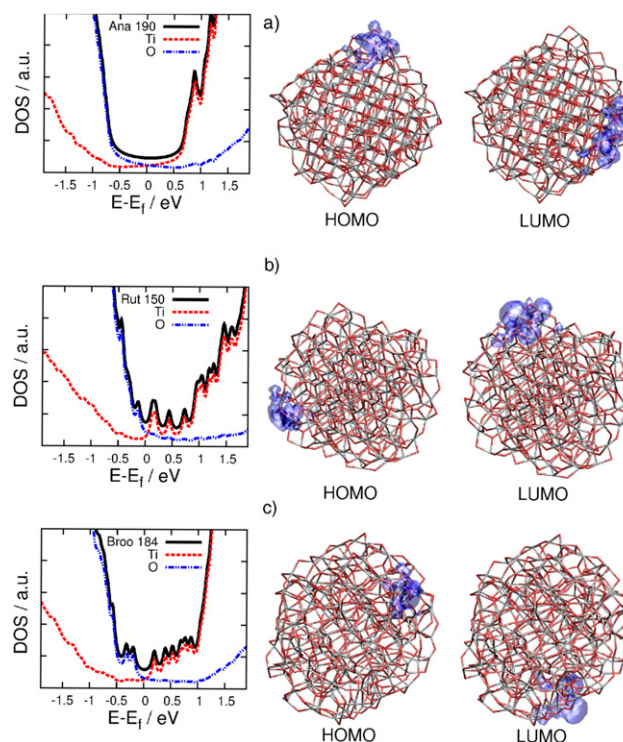
Anatase		Brookite		Rutile	
$N$ TiO <sub>2</sub>	$E_g$ (eV)	$N$ TiO <sub>2</sub>	$E_g$ (eV)	$N$ TiO <sub>2</sub>	$E_g$ (eV)
34	$2.92 \pm 0.28$	40	$3.03 \pm 0.07$	30	$3.13 \pm 0.11$
74	$3.07 \pm 0.07$	72	$3.08 \pm 0.07$	74	$3.02 \pm 0.07$
90	$3.07 \pm 0.06$	104	$3.10 \pm 0.08$	118	$2.97 \pm 0.02$
190	$3.03 \pm 0.04$	184	$3.05 \pm 0.02$	150	$2.99 \pm 0.03$

The smaller the cluster, the less defined its absorption edge. This is consistent with some calculations suggesting that when particles are very small ( $<15$  TiO<sub>2</sub> units), the  $E_g$  values possess an odd–even oscillation with respect to the number of TiO<sub>2</sub> units [52]. This is probably because the edges of both conduction and valence bands are not well defined, in the sense that there are few states near the edges of both bands, the same as the case for the clusters of the present work.

Moreover, the band edges are composed mainly of surface states that tend to lower the BG. As soon as the cluster size is increased, there are more states present in the edges and, therefore, the linear shape of the absorption rise at the edge is better defined. This can be noticed in the uncertainties of the  $E_g$  values of table 1. For a sufficiently large cluster, the lines of figure 4 should become quasi-vertical as more and more states pile up near both band edges. Such surface states are responsible for masking both the theoretical  $E_g$  value (blue shifted) as obtained by using Brus's formula and the distinction among clusters of different crystal structures. In all cases analyzed here, the thermal disorder of the surface hides differences between structural polymorphs and sizes.

Since surfaces of the clusters used in this study are not stabilized by any chemical means, all the particles possess a very high surface energy. This high surface energy comes from the large number of dangling bonds present. These bonds are a source of both low energy excitations and low energy phonons which provide strong thermal fluctuations in the surface structure. This is the main reason for the large amplitudes in fluctuations in  $E_g$  values that mask other effects.

The densities of states (DOS), the projected density of states (pDOS) and the electron density for both the highest occupied molecular orbital (HOMO) and the lowest unoccupied molecular orbital (LUMO) at the DFTB level of theory were calculated for the largest clusters of each type considered in this work, namely, anatase: 190, brookite: 184 and rutile: 150 (see figure 5). It can be observed that both electronic densities are localized on the surface of the nanoparticles, where, in particular, the spatial distributions for the HOMO and LUMO are located on top of the O and Ti atoms, respectively. The surface confinement of the frontier orbital electron densities can be attributed to the presence of dangling bonds in Ti and O surface atoms. A counteracting effect is observed when particles are treated with coating agents where, in this case, electronic densities are found to be delocalized within the clusters [53]. Surface capping agents such as dissociative water will probably modify the absorption spectra calculated here. Including capping agents into the simulations will introduce a lot of arbitrariness, due

**Figure 5.** DOS (solid line), pDOS (dashed lines) and charge density plots of the HOMO and LUMO for: (a) anatase: 190 TiO<sub>2</sub> units; (b) rutile: 150 TiO<sub>2</sub> units; and (c) brookite: 184 TiO<sub>2</sub> units.

to the fact that the anchoring modes are not known for such heterogeneous surfaces (see table S1 in the supporting information available at [stacks.iop.org/JPhysCM/25/000000/mmedia](http://stacks.iop.org/JPhysCM/25/000000/mmedia)). On the other hand, a global geometry optimization of capped TiO<sub>2</sub> NPs would require a great amount of computational effort, even at the DFTB level. The influence of optical properties produced by capping agents in TiO<sub>2</sub> nanoclusters will be the subject of upcoming work.

The structure of the BG for these nanoclusters is revealed by looking at the plots of the DOS depicted in figure 5. The pDOS over the O and Ti atoms are plotted as dashed lines. We can observe that a greater contribution to the valence band comes from O as compared with that from Ti, and the inverse is true for the conduction band. This is in good agreement with previous results [53, 54].

For the case of anatase nanoparticles a clearly defined BG can be seen from the DOS plots of figure 5. On the other hand, rutile and brookite structures show poorly defined BG edges with many localized states within the gap, mainly arising from the dangling bonds of the surface. The study of

surface Ti atoms has demonstrated that the coordination of these atoms is lower than in the bulk. We can thus infer that undercoordinated Ti is mainly responsible for the presence of electronic levels in the BG (see tables S1 and S2 in the supporting information available at [stacks.iop.org/JPhysCM/25/000000/mmedia](http://stacks.iop.org/JPhysCM/25/000000/mmedia)).

The existence of these states explains the highly reactive character of bare nanostructured TiO<sub>2</sub> [55]. In the hypothetical case of anchoring an electron withdrawing dye in the high electron density region of the HOMO and an electron donor dye in the high electron density region of the LUMO (see figure 5), it could be possible to perform the electron–hole separation with visible light, depending on the absorption spectra of these dyes. Such a theoretical device could be important for photocatalytic applications [55, 56].

### 3. Conclusions

We present an alternative procedure for computing the absorption edge of TiO<sub>2</sub> nanoclusters of different sizes and crystal structures. Such clusters were obtained from MD simulations. Values of  $E_g$  calculated using this technique are around 3.0 eV for all the structures analyzed and the uncertainty of this value is smaller when the cluster is larger. These results suggest that Brus's formula is no longer applicable at least for the range of sizes analyzed in this work. The adsorption edge does not allow distinguishing among the three polymorphs. Care must be taken when trying to infer BG properties of a cluster from absorption edge features. Common quantum blue shifting could be masked by surface states that tend to narrow the BG. We showed that the chemical instability of cluster surfaces used is the origin of the large  $E_g$  fluctuations.

### Acknowledgments

We acknowledge support by Consejo Nacional de Investigaciones Científicas y Técnicas (CONICET) through grant PIP 112-200801-000983 and ANPCYT through grant Program BID 1728/OC-AR PICT No. 629 and PME-2006-01581. VCF, MBO and CFAN are grateful for studentships from CONICET.

### Q.7 References

- Q.8 [1] Raskin R S 2010 *Polym. Paint Colour J.* **12** 200  
 Q.9 [2] Gupta K, Tripathi V, Ram H and Raj H 2002 *Colourage* **49**  
 [3] Hwang D, Moon J, Shul Y, Jung K, Kim D and Lee D 2003 *J. Sol-Gel Sci. Technol.* **26**  
 [4] Kim J, Shim J, Bae J, Han S, Kim H, Chang I, Kang H and Suh K 2002 *Colloid Polym. Sci.* **280**  
 [5] Popov A, Priezhev A, Lademann J and Myllylae R 2005 *J. Phys. D: Appl. Phys.* **38**  
 [6] Zhang Y, Zhang L, Mo C, Li Y, Yao L and Cai W 2000 *J. Mater. Sci. Technol.* **16**  
 [7] Chen X and Mao S S 2007 *Chem. Rev.* **107** 2891  
 [8] Hagfeldt A, Boschloo G, Sun L, Kloo L and Pettersson H 2010 *Chem. Rev.* **110** 6595  
 [9] Lyon J E, Rayan M K, Beerbom M M and Schlaf R 2008 *J. Appl. Phys.* **104** 073714

- [10] Ramakrishna G and Ghosh H N 2003 *Langmuir* **505**  
 [11] Kuznetsov V N and Serpone N 2009 *J. Phys. Chem. C* **113** 15110–23  
 [12] Naicker P K, Cummings P T, Zhang H and Banfield J F 2005 *J. Phys. Chem. B* **109** 15243  
 [13] Hoang V V 2008 *Nanotechnology* **1** 19  
 [14] Koparde V N and Cummings P T 2008 *J. Nanopart. Res.* **10** 1169  
 [15] Alivisatos A P 1996 *J. Phys. Chem.* **100** 13226  
 [16] Alivisatos A P 1996 *Science* **271** 993  
 [17] Burda C, Chen X, Narayanan R and El-Sayed M A 2005 *Science* **105** 1025  
 [18] Murray C B, Kagan C R and Bawendi M G 2000 *Annu. Rev. Mater. Sci.* **30** 545  
 [19] Anpo M, Shima T, Kodama S and Kubokawa Y 1987 *J. Phys. Chem.* **91** 4305  
 [20] Li Y, White T J and Lim S H 2004 *J. Solid State Chem.* **177** 1372  
 [21] Manorama S V, Madhusudan Reddy K, Gopal Reddy C V, Narayanan S, Rajesh Raja P and Chatterji P R 2002 *J. Phys. Chem. Solids* **63** 135  
 [22] Kormann C, Bahnemann D W and Hofmann M R 1988 *J. Phys. Chem.* **92** 5196  
 [23] Kavan L, Stoto T and Grätzel M 1993 *J. Phys. Chem.* **97** 9493  
 [24] Satoh N, Nakashima T, Kamikura K and Yamamoto K 2008 *Nature Nanotechnol.* **3** 106  
 [25] Brus L E 1983 *J. Chem. Phys.* **79** 5566  
 [26] Serpone N, Lawless D, Khairutdinov R and Pelizzetti E 1995 *J. Phys. Chem.* **99** 16655  
 [27] Gao F 2010 *Inorg. Chem.* **49** 10409  
 [28] Labat F, Baranek P and Adamo C 2008 *J. Chem. Theory Comput.* **4** 341  
 [29] Reyes-Coronado D, Rodríguez-Gattorno G, Espinosa-Pesqueira M E, Cab C, De Coss R and Oskam G 2008 *Nanotechnology* **19** 1  
 [30] Mahmood T, Cao C, Saeed M A, Ahmed M and Hussain T 2012 (*ESciNano*): *Enabling Science and Nanotechnology, Int. Conf.* doi:10.1109/ESciNano.2012.6149648 Q.10  
 [31] Arroyo-de Dompablo M E, Morales-García A and Taravillo M 2011 *J. Chem. Phys.* **135** 054503  
 [32] Chiodo L, Salazar M, Romero A H, Laricchia S, Della Sala F and Rubio A 2011 *J. Chem. Phys.* **135** 244704  
 [33] Thygesen K S and Jacobsen K W 2009 *Methodology* 12301–8 Q.11  
 [34] Dolgonos G, Aradi B, Moreira N H and Frauenheim T 2010 *J. Chem. Theory Comput.* **6** 266  
 [35] Snoeberger R C, Young K J, Tang J, Allen L J, Crabtree R H, Brudvig G W, Coppens P, Batista V S and Benedict J B 2012 *J. Am. Chem. Soc.* **134** 8911–7  
 [36] Wu B, Guo C, Zheng N, Xie Z G and Stucky D 2008 *J. Am. Chem. Soc.* **130** 17563  
 [37] Elstner M, Porezag D, Jungnickel G, Elstner J, Haugk M, Frauenheim T, Suhai S and Seifert G 1998 *Phys. Rev. B* **58** 7260  
 [38] Aradi B, Hourahine B and Frauenheim T 2007 *J. Phys. Chem. A* **111** 5678  
 [39] Oviedo M B, Negre C F A and Sánchez C G 2010 *Phys. Chem. Chem. Phys.* **12** 6706  
 [40] Oviedo M B and Sánchez C G 2011 *J. Phys. Chem. A* **115** 12280–5  
 [41] Yabana K and Bertsch G F 1996 *Phys. Rev. B* **54** 4484  
 [42] Plimpton S 1995 *J. Comput. Phys.* **1** 117  
 [43] Matsui M and Akaogi M 1991 *Mol. Simul.* **6** 239  
 [44] Koparde V N and Cummings P T 2005 *J. Phys. Chem. B* **109** 24280  
 [45] Koparde V N and Cummings P T 2008 *ACS Nano* **2** 1620  
 [46] Zhang H, Chen B, Banfield J F and Waychunas G A 2008 *Phys. Rev. B* **1** 78

- [47] Koparde V N and Cummings P T 2007 *J. Phys. Chem. C* **111** 6920
- [48] Hosaka N, Sekiya T, Fujisawa M and Kurita S 1996 *J. Electron Spectrosc. Relat. Phenom.* **78** 75
- [49] Sánchez C G, Santos E and Schmickler W 2005 *Phys. Rev. B* **71** 073404
- [50] Shevlin S A and Woodley S M 2010 *J. Phys. Chem. C* **114** 17333–43
- [51] Zhai H-J and Wang L-S 2007 *J. Am. Chem. Soc.* **129** 3022
- [52] Qu Z-W and Kroes G-J 2007 *J. Phys. Chem. C* **111** 16808–17
- [53] Iacomino A, Cantele G, Ninno D, Marri I and Ossicini S 2008 *Phys. Rev. B* **78** 075405
- [54] Zhao Z, Li Z and Zou Z 2010 *J. Phys.: Condens. Matter* **22** 175008
- [55] Fujishima A, Kohayakawa K and Honda J 1975 *J. Electrochem. Soc.* **122** 1487
- [56] Odobel F, Le Pleux L, Pellegrin Y and Blart E 2010 *Acc. Chem. Res.* **43** 1063–71

## Queries for IOP paper 451385

*Journal:* JPhysCM  
*Author:* V C Fuertes *et al*  
*Short title:* A theoretical study of the optical properties of nanostructured TiO<sub>2</sub>

---

### Page 1

#### [Query 1:](#)

Author: Please check the author names and affiliations carefully.

---

### Page 1

#### [Query 2:](#)

Author: Please check the third affiliation.

---

### Page 1

#### [Query 3:](#)

Author: Please be aware that the colour figures in this article will only appear in colour in the Web version. If you require colour in the printed journal and have not previously arranged it, please contact the Production Editor now.

---

### Page 1

#### [Query 4:](#)

Author: In several places I have standardized the English somewhat. Please check that I have not inadvertently altered the meaning.

---

### Page 1

#### [Query 5:](#)

Author: Please check whether the section numberings given are correct.

---

### Page 1

#### [Query 6:](#)

Author: Amended wording 'fewer spherical' OK?

---

### Page 6

#### [Query 7:](#)

Author: Please check the details for any journal references that do not have a blue link as they may contain some incorrect information. Pale purple links are used for references to arXiv e-prints.

---

### Page 6

#### [Query 8:](#)

Author: Please check the journal title given in Ref. [1].

---

### Page 6

#### [Query 9:](#)

Author: [2-6, 10]: Please provide page/article number.

---

### Page 6

#### [Query 10:](#)

Author: [30]: Please provide volume and page/article number.

---

### Page 6

#### [Query 11:](#)

Author: [33]: Please provide volume number.